

# CHARACTERIZING DROPLET COMBUSTION OF PURE AND MULTI-COMPONENT LIQUID FUELS IN A MICROGRAVITY ENVIRONMENT

N 9 3 - 2 0 2 1 9

Gregory S. Jackson and C. Thomas Avedisian  
Sibley School of Mechanical and Aerospace Engineering  
Cornell University  
Ithaca, New York 14853

## Introduction

The importance of understanding the effects of fuel composition, length scales, and other parameters on the combustion of liquid fuels has motivated the examination of simple flames which have easily characterized flow fields and hence, the potential of being modeled accurately. One such flame for liquid fuel combustion is the spherically symmetric droplet flame which can be achieved in an environment with sufficiently low gravity (i.e., low buoyancy). To examine fundamental characteristics of spherically symmetric droplet combustion, a drop tower facility has been employed to provide a microgravity environment to study droplet combustion. This paper gives a brief review of results obtained over the past three years under NASA sponsorship (grant NAG3 -987).

Important aspects which were studied to characterize the burning of liquid droplets included: 1) droplet burning rate constants ( $K$ ) which assess the rate of heat transfer to the liquid fuel from the exothermic gas-phase reactions, 2) extinction of the droplet flame before complete vaporization which indicates the possibility of incomplete combustion, 3) soot formation inside the spherical droplet flame, and 4) microexplosions and preferential vaporization exhibited by multi-stage combustion for droplets of miscible mixtures. The spherically symmetric configuration of microgravity droplet combustion allows for parameters such as average burning rates, flame stand-off ratios, and location of soot agglomerates in the flame to be defined without the effects of natural convective flows, and effects of droplet size in microgravity combustion are not masked by the length scale dependence of natural convective flows.

A wide range of pure and blended fuels were studied in air at standard room temperature and pressure in a low gravity environment on board the drop tower. Results from some of these fuels are briefly reviewed here: pure n-heptane, pure 1-chloro-octane, heptane/monochloro-octane mixtures, pure methanol, methanol/toluene mixtures, and methanol/dodecanol mixtures. The bulk of experimental results reported here were obtained by studying free unsupported droplets with initial diameters ( $D_0$ ) ranging from 0.4 to 0.7 mm. A more limited series of experiments were carried out on fiber-suspended droplets, with  $D_0$  up to 1.1 mm, to examine the effect of initial diameter on the burning of sooting fuels. Different mixture compositions were burned to assess the effects of additives on soot emissions, extinction, and microexplosions.

## Experimental Set-up and Data Extraction

The original drop tower facility as well as the technique for creating free-floating stationary droplets has been described in detail previously [ref. 1, 2]. Many modifications were implemented over the past three years to improve the quality of data obtained from the experiments [refs. 3, 4, 7]. The experimental package contains a combustion chamber with the droplet generator, ignition circuitry, a high-speed movie camera, and a low-lux CCD camera for visualization of the flame boundary. The drop package experiences free fall for about 1.2 s. Some previous experiments showed that the increase in gravity levels in the latter half of free fall due to air drag around the package increased buoyant flows around larger droplets with  $D_0 > 0.80$  mm [ref. 3]. Thus, in order to observe spherically symmetric combustion for the longer-burning larger droplets, a drag shield was built in which the experimental package can fall freely with minimal air drag for the entire period of free fall.

Two types of burning droplet experiments were performed in the drop tower: free unsupported droplets and fiber-suspended droplets. To effectively levitate unsupported droplets in microgravity, a droplet deployment technique based on the "ink jet" method was employed [refs 1, 7]. For the suspended droplets, a 30 to 50  $\mu\text{m}$  diameter quartz

fiber was used. The fiber diameter was kept very small in order to minimize its influence on the burning process. Unsupported droplet experiments reported here included the following fuels: n-heptane, methanol, methanol/toluene mixtures, and methanol/dodecanol mixtures. Suspended droplet experiments reviewed here include pure heptane, pure monochloro-octane, and monochloro-octane/heptane mixtures. Because suspended n-heptane droplets had burning rates and flame stand-off ratios which agreed well with burning rates and flame stand-off ratios of similarly-sized unsupported droplets, the fiber was assumed to have a negligible impact on the combustion process.

Droplets were ignited about 15 ms after the package was released into free fall by two spark discharges on opposite sides of the droplet. Considerable efforts were spent to develop a multiple spark circuit with the capability of adjusting the spark energy, which was controlled by varying the spark duration, the voltage of the energy-storing capacitors, and/or the current through the electrodes. The electrodes for the spark were retracted away from the flame after ignition. Retraction was initially performed by a solenoid-activated spring mechanism which retracted the entire electrode mount upwardly [ref. 3, 5, 7], but more recent experiments have used a mechanism where only the electrodes are retracted in a radially outward direction [ref. 4].

Droplet diameter measurements were obtained from the high-speed movie records with framing rates ranging from 100 to 250 frames per second. Measurements were taken with a computer-based image analysis system (Image Analyst™, Automatix Inc., Billerica, MA). For suspended droplets, measurements were not taken when the average droplet diameter became less than 8 times the nominal fiber diameter because of concerns about the influence of the fiber on the burning process when the fiber diameter becomes a significant fraction of the droplet diameter. The region for calculating the average droplet radius for the suspended droplets was defined as lying between the locations where the liquid surface changed concavity near the fiber, both at the top and at the bottom of the droplet.

## Results and Discussion

### Heptane, Monochloro-octane, and Heptane/Monochloro-octane Mixtures

Burning rate constants were found for unsupported and suspended n-heptane droplets with  $D_0$  ranging from 0.40 to 1.05 mm and for suspended 1-chloro-octane droplets with  $D_0$  from 0.45 to 1.10 mm [ref. 3 - 5]. N-heptane droplets larger than 0.9 mm and 1-chloro-octane droplets larger than 0.8 mm had burning times longer than the duration of free-fall. However, enough of the burning history was recorded for these larger droplets to get a reasonable assessment of  $K$  during the period of so-called steady burning after the initial heat-up period. Representative examples of droplet diameter-squared profiles for unsupported n-heptane droplets are shown in fig. 1. Burning rate constants were found with a least-squared linear regression of the droplet diameter-squared data vs. time. Data from the initial period of droplet heat-up and gas-phase vapor accumulation were excluded from the linear regression. The differences in the slopes of the two profiles in fig. 1 reflect a decreased burning rate for the larger n-heptane droplets. For both n-heptane and monochloro-octane droplets with  $D_0$  around 0.60 mm,  $K$  consistently had values which were more than 20% higher than those for droplets with  $D_0$  around 1.00 mm.

Both heptane and monochloro-octane droplets exhibited common trends in the development of the flame and a shell-like structure of soot (i.e., soot shell) between the droplet and the flame. Soot particles form rapidly enough for all but the smaller-sized heptane droplets, such that thermophoretic forces overtake outward inertia created from the Stefan flow and the particles are pushed inward to a region where the thermophoretic forces balance the outwardly directed drag forces. The soot shell begins to take shape as new particles collect in this region. As burning progresses, the particles begin to agglomerate and the large soot agglomerates are eventually pushed away from the droplet and into the flame zone because the outward drag force increases more rapidly with particle size than does the thermophoretic force [ref. 3]. The soot agglomerates generally escape the flame without complete oxidation implying a loss in heat generation due to unoxidized carbon. As vaporization is completed, the contracting flame passes through and disrupts the remaining soot.

Fig. 2 shows two representative photographic sequences of n-heptane droplets burning at low gravity: an unsupported droplet with  $D_0 = 0.69$  mm and a suspended droplet with  $D_0 = 0.75$  mm. The two sequences have approximately the same  $t/D_0^2$  values to provide some basis for comparison and to show the similarities between the unsupported droplet flames and the suspended droplet flames. The bright particles in fig. 2 are radiating soot particles emitted from the flame without undergoing complete oxidation. The fiber-supported droplet sequence shows some soot agglomerates collecting on the fiber, perhaps due to thermophoresis. However, because burning rates and dimensionless soot shell diameters for fiber-supported droplets agreed well with those of unsupported droplets of similar initial size, the effect on burning of the soot/fiber interactions was assumed to be negligible.

The smaller heptane droplets did not show any soot shell formation until near the end of burning, perhaps due to their higher vaporization rates and the lower residence times for fuel particles inside the flame. On the other hand, the larger heptane droplets ( $D_0 > 0.6$  mm) formed soot shells early in the combustion process and emitted soot agglomerates as combustion proceeded until the end of burning. The smaller monochloro-octane droplets exhibited soot shell development, but their soot structures were much less dense and their emissions greatly reduced in comparison to the larger monochloro-octane droplets.

The flame luminosity, soot emissions, and burning rates of 25%, 50%, and 75% v/v heptane in monochloro-octane suspended droplets fell between those of the two pure components [ref. 3]. The photographic records suggest that more than 25% v/v heptane must be added to monochloro-octane before soot emissions are noticeably reduced as the 25% heptane mixture droplets appeared to soot almost as heavily as pure monochloro-octane droplets of similar size. No multi-stage combustion process was observed for these mixtures.

Photographic records of the pure heptane and monochloro-octane droplets suggest that the amount of soot collected in the shell and unoxidized by the flame may be a more sensitive function of the droplet diameter than a  $D^2$  dependence. Longer residence time for fuel molecules inside the droplet flame should promote fuel pyrolysis and soot production. An approximate estimate for the residence time of fuel molecules inside the flame is obtained by integrating with respect to radial position the inverse of the average velocity of fuel molecules inside the flame. This residence time can be shown to scale with  $D^2$  [ref. 3]. Therefore, larger droplets have more time for fuel pyrolysis and soot formation. A large amount of soot formation early in the combustion process of large droplets may encourage further soot formation by surface reactions on newly-formed soot particles. If the amount of soot formed is more sensitive to droplet diameter than  $D^2$ , proportionately more carbon atoms from the vaporized fuel goes into forming soot for larger droplets than for smaller droplets. This lowers the proportionate amount of heat released for droplet vaporization and the corresponding burning rate constant.

#### Methanol and Methanol/Toluene Mixtures

Experimental results of pure methanol droplets showed that methanol droplets produce virtually non-luminous flames in microgravity at atmospheric pressure [ref. 6]. Pure toluene droplets, however, have been shown to produce highly sooting flames with the formation of dense soot shells between the droplet and the flame [ref. 1, 5]. Furthermore, pure methanol droplets exhibit flame extinction, attributed to water vapor absorption into the liquid phase, and pure toluene droplets have been shown to emit large quantities of soot due to the break-up of the soot shell near the end of burning. These differences in the behavior of methanol and toluene motivated the study of mixture droplets of these two fuels [ref. 7] in order to ascertain whether some of the less favorable characteristics of the spherically symmetric combustion of the pure components could be eliminated. Pure methanol droplets were burned in the microgravity environment in order to provide a basis for comparison with the mixtures which included 5%, 25%, and 50% v/v toluene in methanol.

Pure methanol droplets with  $D_0$  from 0.40 to 0.45 mm burned with a faint non-luminous flame and exhibited extinction at droplet diameters ranging from 160 to 190  $\mu\text{m}$ . 5% v/v toluene in methanol droplets, with  $D_0$  ranging from 0.5 to 0.6 mm, burned without any observable difference from the pure methanol droplets. The flame did not appear luminous or exhibit soot formation. Average  $K$  values of the 5% toluene droplets before extinction matched those for pure methanol droplets, and extinction of the 5% toluene droplets consistently occurred at droplet diameters similar to those of pure methanol droplets. In fact, all toluene/methanol droplets had similar droplet diameter-squared profiles as shown by the sample in fig. 3 in spite of tremendous differences in flame luminosity and soot production, demonstrated partly by the photographic sample of the 50% toluene mixture droplet in fig. 4.

Marked increases in the flame luminosity indicating oxidation of soot precursors resulted from the burning of 25% v/v toluene droplets, with  $D_0$  between 0.45 and 0.60 mm. The visibility of the flame increased as combustion proceeded as demonstrated by the two sequences shown in fig. 5. This increase with time may be explained by the fact that the fractional vaporization of toluene increased as combustion proceeded. Furthermore, the intensity of the flame luminosity appeared to be sensitive to droplet size as shown in comparing the two sequences in fig. 5. Nonetheless, the flames for all 25% toluene droplets studied ( $D_0$  between 0.45 and 0.60 mm) did not produce soot agglomerates, which suggests that this mixture might be useful in promoting flame luminosity for methanol-based fuels without soot emissions. However, flame extinction was still observed for this mixture as shown in the characteristic diameter squared profile of fig. 3. Extinction diameters and burning rate constants before extinction were again similar to those for pure methanol droplets (~ 160 - 180  $\mu\text{m}$ ).

The 50% v/v toluene mixtures burned with a dramatic increase in soot production to the extent that a dense soot shell eventually formed around the droplet and large agglomerates of soot were emitted through the flame near the end of burning, as in the combustion of pure toluene droplets. However, unlike the combustion of pure toluene droplets, the mixture droplets (ranging in  $D_0$  from 0.45 to 0.55 mm) burned with an initial stage of low luminosity, which suggests an initial period where the fractional vaporization of toluene is low. As methanol is preferentially removed from the droplet surface in the early period of combustion, the fractional vaporization of toluene increases to eventually cause the rapid production of soot particles in the gas phase, demonstrated in the photographs of fig. 4. The soot particles rapidly agglomerate and form a soot shell around the droplet much like the heptane and monochloro-octane droplets mentioned above. The collapse of the flame near the end of burning results in the disruption of the soot shell. The flame extinguishes before the droplet is completely vaporized. The size of the remaining droplets after the collapse of the flame is clearly smaller ( $< 140 \mu\text{m}$ ) than the extinction diameter of the other two methanol/toluene mixtures studied. The differences in the behaviors of the 50% toluene droplets can in part be explained by vapor/liquid equilibrium data for methanol and toluene which shows that the 50% toluene mixture lies on the toluene rich side of a negative azeotrope for methanol/toluene mixtures [ref. 7].

#### Methanol/Dodecanol Mixtures

Adding dodecanol to methanol resulted in different droplet combustion behavior than with adding toluene to methanol. 25% v/v and 50% v/v dodecanol in methanol mixture droplets were burned in the low-gravity environment. The following burning characteristics of the methanol/dodecanol mixture droplets, with  $D_0$  ranging from 0.50 to 0.60 mm, were observed [ref. 6]: 1) droplet burning appeared to be a multi-stage process for both mixture compositions studied, 2) microexplosions were observed for some of the 25% dodecanol droplets, and 3) extinction did not occur for the mixtures.

Multi-stage combustion in mixture droplets is characterized by a period midway through combustion when the droplet diameter remains relatively constant as its temperature rises and the liquid density correspondingly decreases due to the fractional vaporization of the less volatile component. Such a period is clearly evident in the  $D^2$  profiles for both the 50% v/v and a 25% v/v dodecanol in methanol mixture droplets in fig. 6. The multi-stage combustion for the methanol/dodecanol droplets is caused by diffusion-controlled vaporization where the more volatile methanol gradually is depleted at the droplet surface and cannot be replenished fast enough at the surface due to slow liquid-phase diffusion. The droplet volume reduction before the intermittent period of heating (e.g., ~25% for the 50% methanol mixture) leaves some methanol in the droplet interior, and thus in the final stage of combustion both dodecanol and methanol are being vaporized.

Microexplosions did not occur for the 50% dodecanol droplets burning in microgravity, while microexplosions were observed for over two thirds of the 25% dodecanol droplets. Microexplosions were characterized by the rapid formation and expansion of a bubble within the droplet, which eventually bursts as shown in fig. 7. The initiation of microexplosion is caused by the droplet temperature reaching the superheat limit as discussed in ref. 6.

Methanol/dodecanol mixtures cannot attain temperatures higher than the boiling point of dodecanol during burning. Therefore, any methanol/dodecanol mixture composition with a superheat limit above the dodecanol boiling point will not undergo microexplosion. Calculation of methanol/dodecanol mixture superheat limits at one atmosphere showed that the 50% dodecanol mixture had a superheat limit that was too high for microexplosion while the 25% dodecanol mixture superheat limit was slightly lower than the dodecanol boiling point [ref. 7]. This sheds light on the experimental results which showed microexplosion for only two thirds of the 25% dodecanol mixture droplets. Because the 25% dodecanol mixture has a superheat limit near the boiling point of dodecanol, it is not surprising that some 25% dodecanol droplets did not exhibit microexplosion.

The addition of dodecanol to methanol was found to suppress extinction exhibited as all the 50% dodecanol and non-exploding 25% dodecanol mixture droplets appeared to burn to completion. Water absorption within the droplet may be insignificant during combustion of these mixture droplets because of the higher droplet surface temperatures and the lower solubility of water in dodecanol.

#### Conclusions

The microgravity environment has proven a very useful tool in examining different aspects of droplet combustion. The spherically symmetric droplet flames simplified the interpretation of all of these phenomena because the interactions between the liquid and the gas-phase were more clearly defined. These aspects included: 1) an influence of droplet size on soot formation in heptane and monochloro-octane droplets, 2) the possibility that

increased soot formation and emissions of larger droplets encourage a decrease in the burning rate constant with initial droplet size for sooting fuels, 3) the usefulness of mixing methanol and toluene to achieve a luminous droplet flame without soot emissions, 4) microexplosions of methanol/dodecanol mixture droplets, and 5) the potential of mixing a heavier alcohol (such as dodecanol) with methanol to suppress flame extinction exhibited by pure methanol droplet. Future work will seek to further quantify the influence of soot on the burning process and to examine a wide range of fuel mixtures.

### References

1. Avedisian, C.T., Yang, J.C., and Wang, C.H., "On low gravity droplet combustion", *Proc. R. Soc. Lond.* **A420**, 1988, pp. 183-200.
2. Yang, J.C., An experimental method for studying combustion of an unsupported fuel droplet at reduced gravity, Ph.D. thesis, Cornell University, Ithaca, New York, 1990.
3. Jackson, G.S., Avedisian, C.T., and Yang, J.C., "Observations of Soot during Droplet Combustion at Low Gravity: Heptane and Heptane/Monochloro-alkane Mixtures", *Int. J. Heat Mass Trans.* **35** (8), 1992, pp. 2017-2033.
4. Jackson, G.S. and Avedisian, C.T., "Experiments on the Effect of Initial Diameter in Spherically Symmetric Droplet Combustion of Sooting Fuels", Paper no. 93-0130, AIAA 31st Aerospace Sciences Meeting, Reno, Nevada, 1993.
5. Jackson, G.S. and Avedisian, C.T., "Possible Effect of Initial Diameter in Spherically Symmetric Combustion of Sooting Fuels", Paper no. 110, Eastern States Section Meeting of the Combustion Institute, Ithaca, NY, October, 1991.
6. Yang, J.C., Jackson, G.S., Avedisian, C.T., Combustion of unsupported methanol/dodecanol mixture droplets at low gravity, *Twenty-Third Symp. (Int.) on Comb.*, The Combustion Institute, Pittsburgh, 1990, pp. 1619-1625.
7. Jackson, G.S., Avedisian, C.T., and Yang, J.C., "Soot Formation During Combustion of Unsupported Methanol/Toluene Mixture Droplets in Microgravity", *Proc. R. Soc. Lond.* **A435**, 1991, pp. 359-369.

### Figures

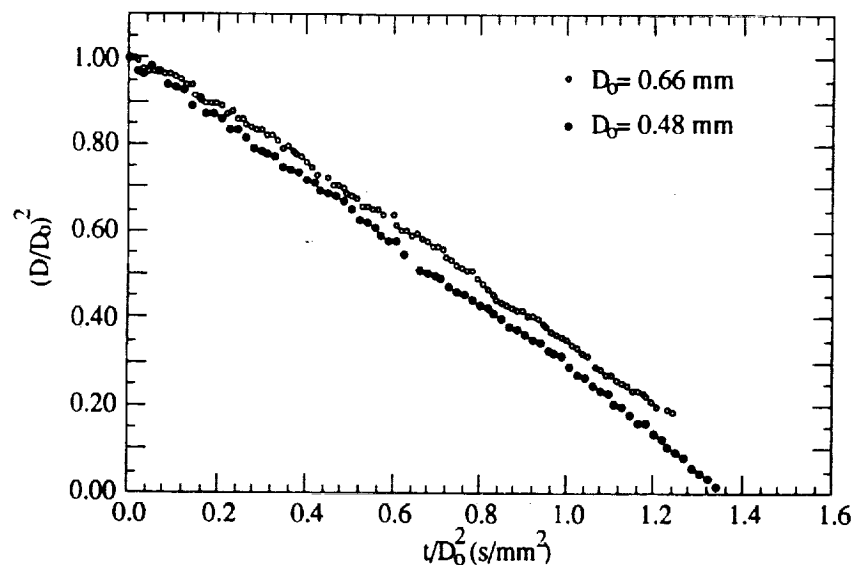
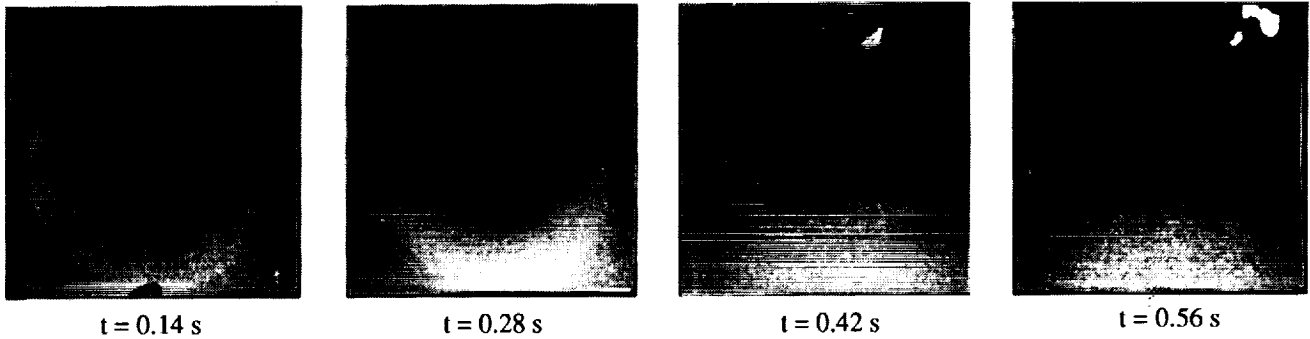


Figure 1. -- Two examples of dimensionless diameter-squared profiles for unsupported heptane droplets burning in microgravity [ref. 4].

$D_0 = 0.69$  mm, unsupported



$D_0 = 0.75$  mm, supported

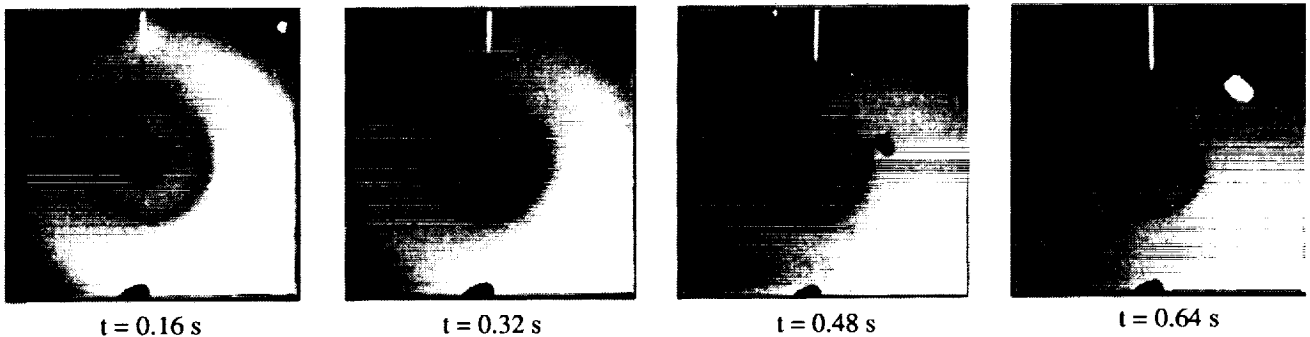


Figure 2. -- Comparison of unsupported and suspended heptane droplets burning in microgravity [ref. 4].

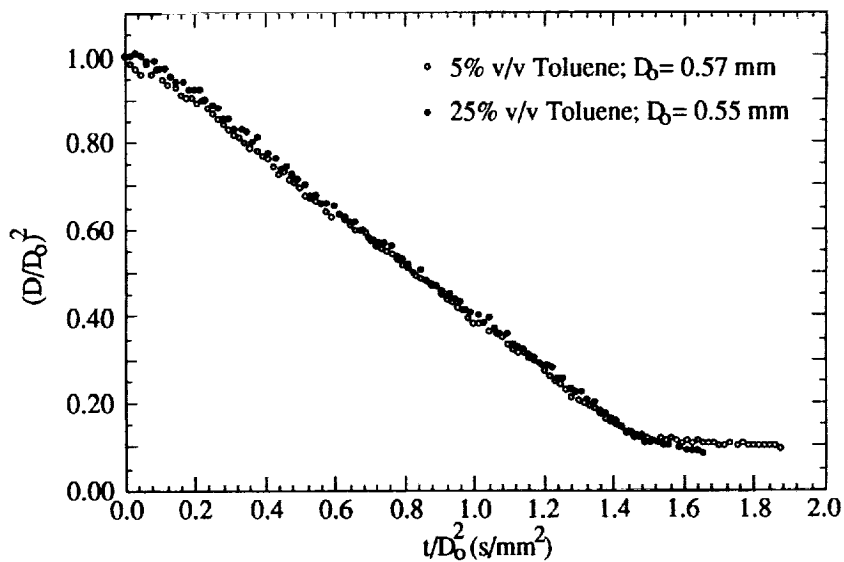


Figure 3. -- Dimensionless diameter-squared profiles for two methanol/toluene mixture droplets burning in microgravity [ref. 7].

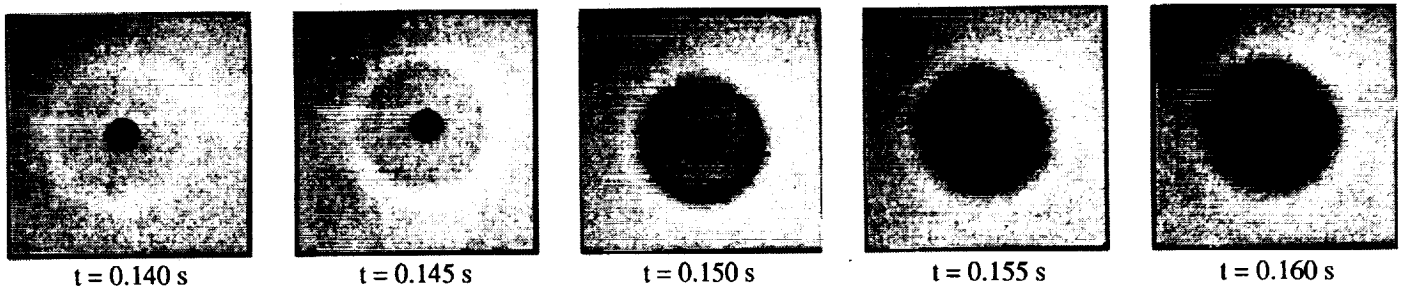
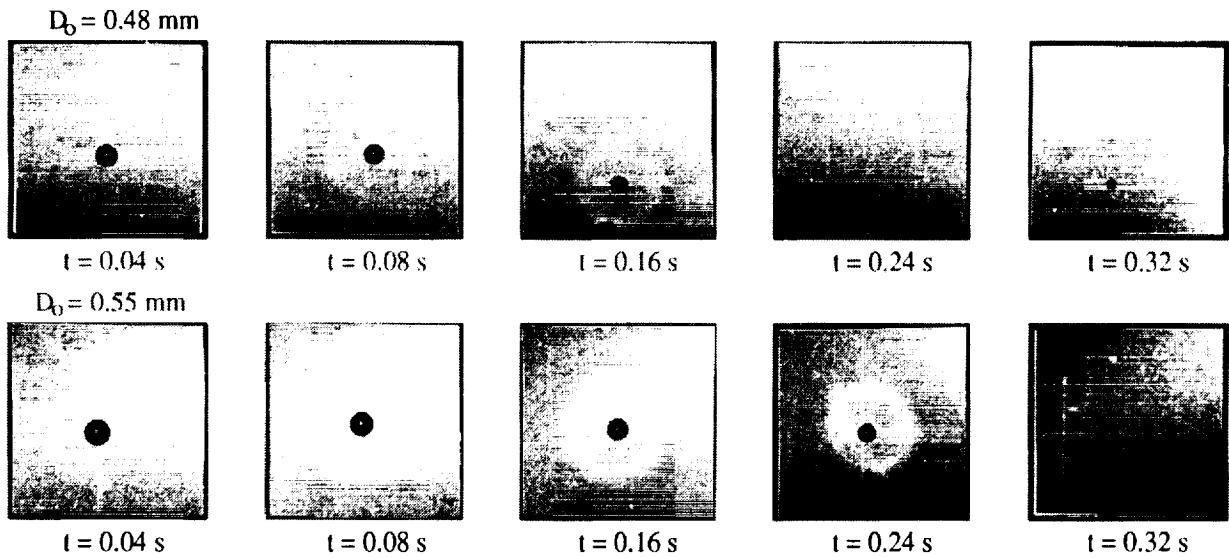
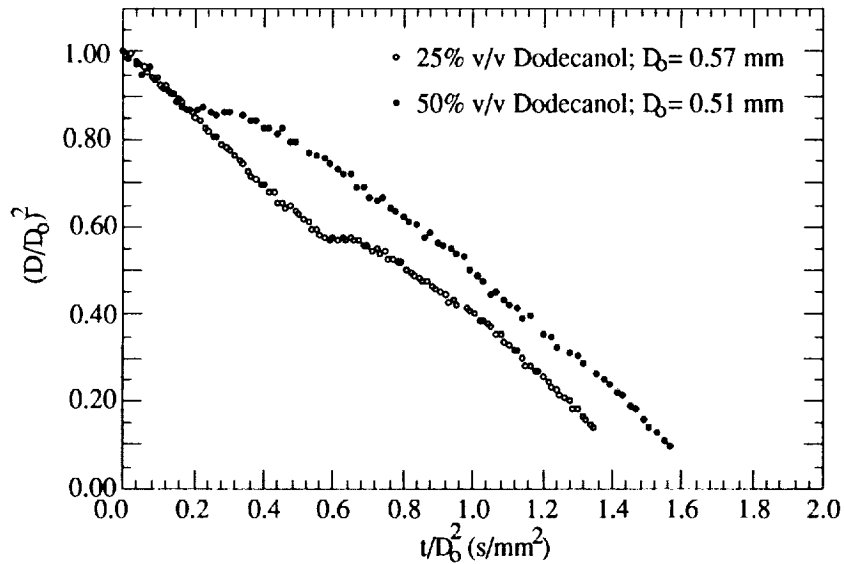


Figure 4. -- 50% v/v toluene in methanol droplet burning at low gravity, exhibiting rapid formation of soot [ref. 7].



**Figure 5.** -- Comparison of flame luminosity of two 25% v/v toluene in methanol droplets with different initial diameters burning in microgravity [ref. 7].



**Figure 6.** -- Dimensionless diameter-squared profiles for two methanol/dodecanol droplets burning in microgravity illustrating multi-staged combustion.

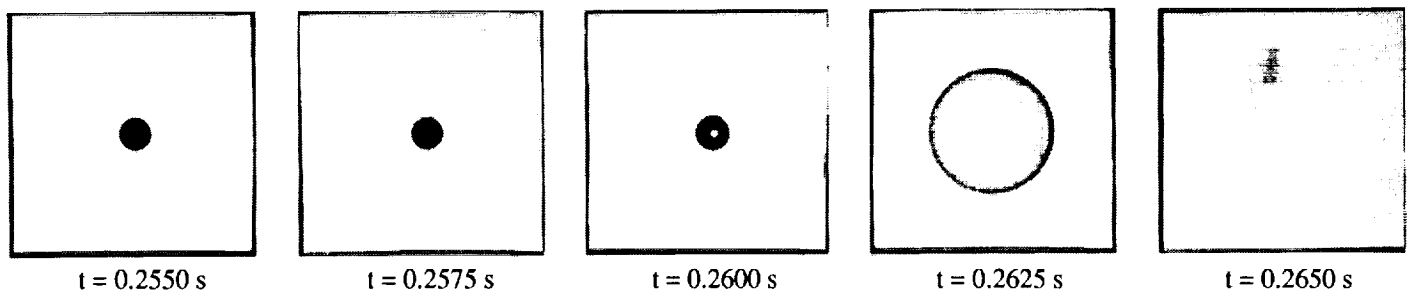


**Figure 7.** -- 75% v/v methanol in dodecanol droplet burning in microgravity which illustrates microexplosion [ref. 6].

